Apoptosis (2019) 24:359–368
https://doi.org/10.1007/s10495-019-01525-z

Eukaryotic elongation factor 2 (eEF2) kinase/eEF2 plays protective roles against glucose deprivation-induced cell death in H9c2 cardiomyoblasts

Satoshi Kameshima[1] · Muneyoshi Okada[1] · Hideyuki Yamawaki[1]

Published online: 8 February 2019

Abstract
During the development of cardiac hypertrophy, glucose deprivation (GD) associated with coronary microvascular rarefaction is caused, leading to cardiomyocyte death. Phosphorylation (inactivation) of eukaryotic elongation factor 2 (eEF2) by eEF2 kinase (eEF2K) inhibits protein translation, a highly energy consuming process, which plays protective roles against nutrient deprivation-induced cell death. We previously showed that eEF2 phosphorylation was increased in isolated heart from several cardiac hypertrophy models. In this study, we investigated whether eEF2K/eEF2 mediates the inhibition of cardiomyocyte death under GD condition. In H9c2 rat cardiomyoblasts cultured with serum-free medium, GD significantly augmented eEF2 phosphorylation and signals related to autophagy [increase of microtubule-associated protein 1 light chain 3 (LC3)-II to LC3-I ratio] and apoptosis (cleavage of caspase-3) as determined by Western blotting. GD induced cell death, which was augmented by eEF2K gene knockdown using a small interfering RNA. eEF2K gene knockdown significantly augmented GD-induced cleavage of caspase-3 and apoptotic nuclear condensation as determined by 4′, 6-diamidino-2-phenylindole staining. In contrast, eEF2K gene knockdown significantly inhibited GD-induced increase of LC3-II to LC3-I ratio and autophagosome formation as determined by an immunofluorescence staining. An inhibitor of autophagy, 3-methyladenine or bafilomycin A1 significantly augmented GD-induced cleavage of caspase-3. Further, eEF2K gene knockdown significantly inhibited GD-induced phosphorylation of adenosine monophosphate-activated protein kinase (AMPK)α and its downstream substrate, unc-51 like autophagy activating kinase (ULK)1. An inhibitor of AMPK, dorsomorphin significantly inhibited GD-induced increase of LC3-II to LC3-I ratio. In conclusion, we for the first time revealed that eEF2K/eEF2 axis under GD condition mediates the inhibition of apoptotic H9c2 cell death at least in part via promotion of autophagy through AMPKα/ULK1 signaling pathway.

Keywords Adenosine monophosphate-activated kinase · Apoptosis · Autophagy · Cardiac hypertrophy · Eukaryotic elongation factor 2 · Glucose deprivation

Introduction

Cardiac hypertrophy is one of the compensation mechanisms against the circulatory insufficiency including hypertension [1], valvular heart disease [2] and cardiomyopathy [3]. However, decrease of coronary microvascular density and the following deprivation of nutrients including glucose in cardiomyocytes are caused during the development of cardiac hypertrophy, which leads to cardiomyocyte death and cardiac dysfunction [4, 5]. Glucose deprivation (GD) was reported to induce apoptosis in several types of cells including cardiomyocytes [6, 7]. Autophagy is a highly conserved intracellular process for protein degradation and recycling, which was reported to play protective roles against the

Electronic supplementary material The online version of this article (https://doi.org/10.1007/s10495-019-01525-z) contains supplementary material, which is available to authorized users.

✉ Hideyuki Yamawaki
yamawaki@vmas.kitasato-u.ac.jp

[1] Laboratory of Veterinary Pharmacology, School of Veterinary Medicine, Kitasato University, Higashi 23 bancho 35-1, Towada, Aomori 034-8628, Japan

apoptotic cell death under nutrient-deprived condition. In mouse neuroblastoma cell line, an inhibitor of autophagy, bafilomycin A1 (Baf A1) or 3-methyladenine (3-MA), augments the expression of apoptosis-related molecules induced by GD and the following glucose reperfusion [8]. In addition, estradiol was reported to inhibit apoptotic osteoblast death via the promotion of autophagy under serum-deprived condition [9].

Protein translation is a highly energy consuming process, which is positively regulated by eukaryotic elongation factor 2 (eEF2) in eukaryotes. eEF2, a 95.2 kDa protein consisting of 857 amino acids, belongs to the G-protein superfamily and promotes guanosine triphosphate-dependent translocation of peptidyl-tRNA from the A to P site in ribosome [10]. eEF2 is phosphorylated and inactivated by its specific upstream kinase, eEF2 kinase (eEF2K). It was reported in several tumor cells that eEF2K/eEF2 axis mediates an increase of cell viability through the inhibition of energy consumption via decreasing protein translation under nutrient-deprived condition [11]. We previously showed that eEF2K activation and the following eEF2 phosphorylation were increased in the isolated heart from several cardiac hypertrophy models [12]. In this study, we thus tested the hypothesis that eEF2K/eEF2 plays protective roles in the cell death under GD condition, and revealed that the eEF2K/eEF2 axis mediates an inhibition of caspase-3-dependent apoptosis at least in part via the promotion of autophagy in the glucose-deprived H9c2 cardiomyoblasts.

Methods

Materials

Regent sources were as follows: 3-MA (Calbiochem; Merck, Darmstadt, Germany), dorsomorphin (Adooq Bioscience, Irvine, CA, USA) and Baf A1 (BioViotica, Dransfeld, Germany). 3-MA was dissolved in serum-free culture medium. Dorsomorphin or Baf A1 was dissolved in dimethyl sulfoxide (DMSO; final concentration was 0.1%).

Antibody sources were as follows: phospho-eEF2 (No. 905-775-100) (Assay designs, Ann Arbor, MI, USA); total-eEF2 (No. A301-688A-T) (Bethyl Laboratories, Montgomery, TX, USA); total-eEF2K (No. sc-390710) (Santa Cruz Biotechnology, Dallas, TX, USA); microtubule-associated protein 1 light chain 3 (LC3; No. 2775S), cleaved caspase-3 (No. 9661S), phospho-adenosine monophosphate (AMP)-activated protein kinase (AMPK)α (No. 2535), total-AMPKα (No. 2603), phospho-acetyl-CoA carboxylase (ACC; No. 3661), total-ACC (No. 3676), phospho-unc-51 like autophagy activating kinase (ULK)1 (No. 5869), total-ULK1 (No. 8054) (Cell Signaling Technology, Beverly, MA, USA); total-actin (MAB1501) (Sigma-Aldrich, St. Louis, MO, USA).

Cell culture

H9c2 rat cardiomyoblasts were obtained from American Type Culture Collection (Manassas, VA, USA), and the cells at passage 18–43 were used in this study. The cells were cultured in Dulbecco Modified Eagle's Medium (DMEM; No. 041-29775, Wako, Osaka, Japan) supplemented with 10% fetal bovine serum (Gibco; Thermo Fisher Scientific, Waltham, MA, USA) and a mixture of 1% penicillin–streptomycin (Nacalai tesque, Kyoto, Japan) at 37 °C in 5% CO_2 [13], and used for each experiment at 70–90% confluence. They were exposed for 6–26 h to serum-free DMEM in the absence of glucose (No. 042-32255, Wako, the osmolarity was adjusted for that of the DMEM with glucose) as GD. The cells were treated with dorsomorphin (5 μM) or 3-MA (2 mM) during GD for 12 or 24 h, respectively. Baf A1 (10 nM) was added to the medium 3 h or 6 h before the end of 12 h- or 24 h-GD stimulation.

Small interfering (si)RNA transfection

H9c2 cells at 70–80% confluence were transfected with siRNA against eEF2K (#1: ACUAAAAUCAUGGAC UGCCtt or #2: UGUUGUACCAGUGUAAGGCtt; Nippon Gene, Toyama, Japan) or/and eEF2 (UCGAUCAUG AUAUUGCCCAtt; Nippon Gene) by a lipofection method using ScreenFect siRNA (Wako) at a final concentration of 20 nmol/l. Non-silencing siRNA (#1: Nippon Gene or #2: RNAi inc., Tokyo, Japan) was used as a negative control. Then, the cells were recovered for an additional 24 h before GD stimulation. siRNA with sequence #1 against non-silencing control or eEF2K was used in all the eEF2K gene knockdown studies except for the experiments described in Supplementary Fig. 2 where sequence #2 was used.

Western blotting

Western blotting was performed as described previously [14]. Protein lysates were obtained by homogenizing H9c2 cells with Triton X-100-based lysis buffer, and protein concentration was measured using a bicinchoninic acid method (Pierce, Rockford, IL, USA). Equal amount of proteins (2–14 μg) was separated by SDS-PAGE (7.5–14%) and transferred to a nitrocellulose membrane (Pall, Ann Arbor, MI, USA). After blocked for 1 h with 3% bovine serum albumin, the membrane was incubated with the following primary antibodies: phospho-eEF2 (1:1000 dilution), total-eEF2 (1:2000 dilution), total-eEF2K (1:500 dilution), LC3 (1:500–1000 dilution), cleaved caspase-3 (1:500 dilution), phospho-AMPKα (1:1000 dilution), total-AMPKα (1:500

dilution), phospho-ACC (1:500 dilution), total-ACC (1:500 dilution), phospho-ULK1 (1:500 dilution), total-ULK1 (1:500 dilution) and total-actin (1:1000–3000 dilution) at 4 °C overnight and was visualized using a horseradish peroxidase-conjugated secondary antibody (1:10,000 dilution, 45 min) and the chemiluminescent reagent (EZ-ECL kit; Biological Industries, Kibbutz Beit Haemek, Israel or ECL Prime kit; Amersham; GE healthcare, Marlborough, MA, USA). The resulting bands were analyzed using CS Analyzer 3.0 software (ATTO, Tokyo, Japan). Equal loading of protein was confirmed by measuring expression of each total protein or total-actin.

Cell viability assay

Cell viability was assessed by a cell counting using cell counting kit-8 (Dojindo, Kumamoto, Japan) as described previously [15]. After stimulation of the cells with GD for 24–26 h, the images were taken using a phase contrast microscope (CKX-31, Olympus, Tokyo, Japan) equipped with a digital camera (Bio Medical Science, Tokyo, Japan). After washed with Tris-buffered saline, the cells were incubated for 2 h in serum-free DMEM in the presence of a color reagent at 37 °C. The absorbance of the cultured medium was measured at 450 nm using a standard 96 well plate reader (TriStar LB 941; Berthold Technologies, Bad Wildbad, Germany).

Determination of apoptotic nuclear condensation by 4′, 6-diamidino-2-phenylindole (DAPI) staining

DAPI staining was performed to observe a nuclear morphology as described previously [16]. After stimulation of the siRNA-transfected cells with GD for 24 h, DAPI (1 μg/ml, Dojindo) was added for 5 min at room temperature. The images were taken using a fluorescent microscope (BX-51; Olympus) equipped with a digital camera (DP74; Olympus). The ratio of condensed to total nuclei was calculated (300 cells, shown in %).

Determination of autophagosome formation by an immunofluorescence staining

Autophagosome formation was examined by an immunofluorescence staining using a specific antibody against LC3 [17]. After transfection with siRNA and the following GD stimulation for 12 h, the cells were fixed with 4% paraformaldehyde and permeabilized with 0.2% Triton X-100. After blocked for 1 h with 1% normal goat serum, the cells were incubated with LC3 antibody (1:250 dilution) at 4 °C overnight and visualized using a fluorescent-dye-conjugated secondary antibody (Alexa Fluor 488; Thermo Fisher Scientific). The images were taken using a fluorescent microscope (BX-51) equipped with a digital camera (DP74). The cells with > 10 LC3-positive green fluorescent dots were counted as an autophagic cell, and the ratio to total cells (> 100 cells) in > 10 fields was calculated (shown in %).

Statistics

Data were shown as means ± SEM. Statistical evaluations were performed using one-way ANOVA followed by Bonferroni's post-hoc test (comparison between multiple groups) or unpaired Student's t-test (comparison between two groups). Values of $P < 0.05$ were considered statistically significant.

Results

GD augments phosphorylation (inactivation) of eEF2 and signals related to autophagy and apoptosis in H9c2 cardiomyoblasts

During the development of cardiac hypertrophy, density of coronary microvessel is decreased. The microvascular rarefaction causes deprivation of nutrients including glucose, leading to cardiomyocyte death [4, 5]. It was reported that eEF2 phosphorylation (inactivation) was induced under the nutrient-deprived condition [18]. Therefore, we first examined the effects of GD on eEF2 phosphorylation and the signals related to autophagy and apoptosis in H9c2 cardiomyoblasts cultured with serum-free medium. GD significantly increased eEF2 phosphorylation (GD 6 h; $n = 4$, $P < 0.05$, Fig. 1A). The LC3-II to LC3-I ratio (GD 12 h; $n = 8$, $P < 0.01$, Fig. 1B) and the expression of cleaved caspase-3 (GD 24 h; $n = 4$, $P < 0.01$, Fig. 1C) were significantly increased by GD. We next examined by using an inhibitor of autophagy, Baf A1 whether the autophagic flux was promoted by GD in H9c2 cells cultured with serum-free medium. We found that Baf A1 augmented GD-induced increase of LC3-II to LC3-I ratio ($n = 3$, Supplementary Fig. 1), indicating that GD promoted the autophagic flux in H9c2 cells. In addition, GD (24 h) significantly decreased cell viability ($n = 6$, $P < 0.01$, Fig. 1D, E).

eEF2K gene knockdown increases apoptotic cell death under GD condition

Protein translation is a highly energy consuming process, which is promoted by eEF2 activation. In GD condition, energy consumption is one of the causes for cell death. Thus, we tested the hypothesis that GD-induced eEF2 inactivation (phosphorylation) mediated by its specific upstream kinase, eEF2K plays a protective role in cell death by using a knockdown technique. We confirmed that eEF2K gene knockdown by transfection with a specific siRNA decreased the

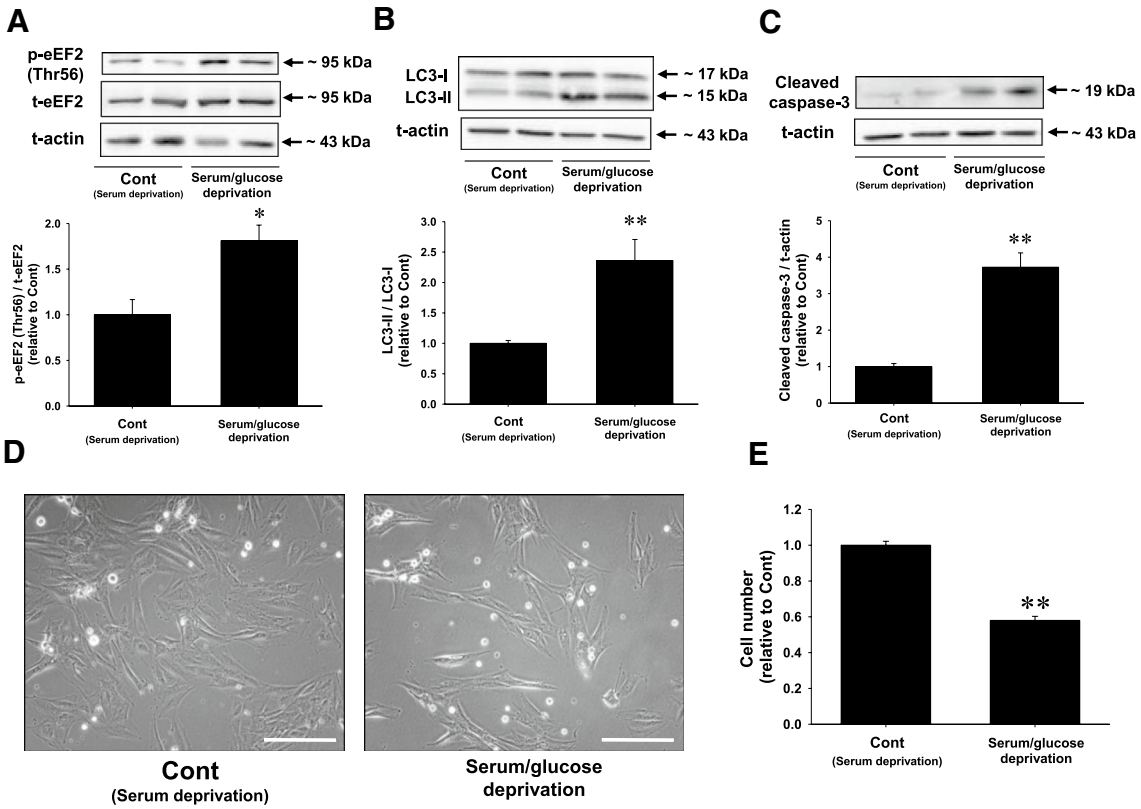

Fig. 1 Glucose deprivation (GD) augments phosphorylation (inactivation) of eukaryotic elongation factor 2 (eEF2) and signals related to autophagy and apoptosis in H9c2 cardiomyoblasts. H9c2 cells were incubated with serum-free medium in the presence (Cont) or absence of glucose for 6–24 h. After extraction of proteins, expression levels of phospho- or total-eEF2 (GD 6 h, n = 4; **A**), microtubule-associated protein 1 light chain 3 (LC3; GD 12 h, n = 8; **B**) and cleaved caspase-3 (GD 24 h, n = 4; **C**) were determined by Western blotting. Phospho-eEF2 (p-eEF2) or cleaved caspase-3 was normalized to total-eEF2 (t-eEF2) or total-actin (t-actin), respectively. Ratio of LC3-II to LC3-I was measured as a quantitative index of autophagy. The results were shown as fold increase relative to Cont. Effects of GD on H9c2 cell viability were examined by a cell counting using colorimetric method. Representative photomicrographs were shown (**D**; n = 6), and the result was shown as fold increase relative to Cont (**E**; n = 6). $^{*}P < 0.05$, $^{**}P < 0.01$ vs. Cont. Scale bar: 100 μm

eEF2K protein expression (n = 3, Fig. 2A) and GD-induced eEF2 phosphorylation (GD 6 h; n = 5 Fig. 2A). eEF2K gene knockdown augmented GD-induced cell death (GD 26 h, n = 7, Fig. 2B). We next examined the effects of eEF2K gene knockdown on GD-induced apoptosis. In control siRNA-transfected cells, GD (24 h) significantly increased apoptotic nuclear condensation (n = 5, $P < 0.01$, Fig. 3A, B), which was significantly augmented by eEF2K gene knockdown (n = 5, $P < 0.01$, Fig. 3A, B). Moreover, eEF2K gene knockdown significantly increased GD-induced cleavage of caspase-3 (n = 6, $P < 0.01$, Fig. 3C, n = 3, $P < 0.01$, Supplementary Fig. 2).

eEF2K gene knockdown inhibits GD-induced autophagy

Autophagy is a highly conserved intracellular process for protein degradation and recycling in eukaryotic cells. We next examined the effects of eEF2K gene knockdown on GD-induced autophagy in H9c2 cells. In the progression of autophagy, a double-membrane vesicle, autophagsome is formed. Since LC3 proteins are contained in autophagosomal membrane, autophagosomes can be detected as an intracellular fluorescent dot (punctate LC3) by an immunofluorescence staining using a specific antibody against LC3 [17]. In control siRNA-transfected cells, GD (12 h) significantly increased the number of punctate LC3-positive cells, which was significantly inhibited by eEF2K gene knockdown (n > 100 cells in > 10 fields from each stimulation of three independent experiments, $P < 0.01$, Fig. 4A, B). Moreover, eEF2K gene knockdown significantly inhibited GD-induced increase of LC3-II to LC3-I ratio (n = 5, $P < 0.01$, Fig. 4C).

eEF2K/eEF2 axis under GD condition inhibits apoptosis via promoting autophagy

We next performed eEF2 gene knockdown study in order to elucidate whether the activation (dephosphorylation)

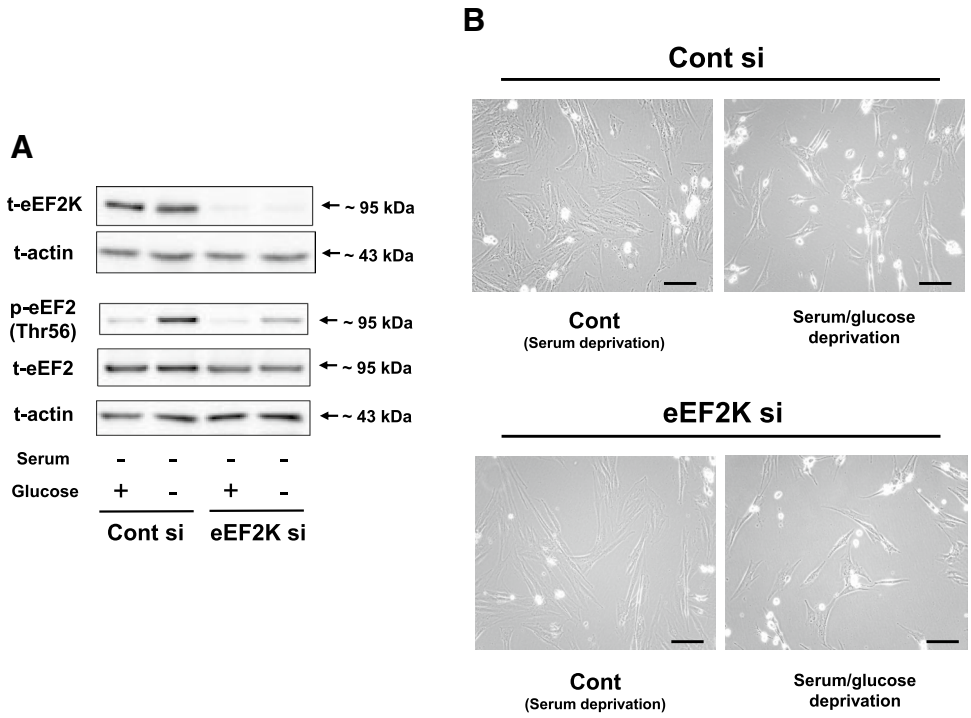

Fig. 2 Effects of gene knockdown of eEF2 kinase (eEF2K), a specific upstream kinase for eEF2, on GD-induced H9c2 cardiomyoblast death. After transfection with a specific small interfering (si) RNA against eEF2K (eEF2K si) or a non-silencing control siRNA (Cont si), H9c2 cells were incubated with serum-free medium in the presence or absence of glucose for 6–26 h. After extraction of proteins, expression levels of total-eEF2K (t-eEF2K) and p-eEF2 (GD 6 h) were determined by Western blotting. Equal protein loading was confirmed using t-actin antibody. Representative images were shown (**A**; n = 3–5). Effects of eEF2K gene knockdown on GD (26 h)-induced cell death were examined. Representative photomicrographs were shown (**B**; n = 7). Scale bar: 100 μm

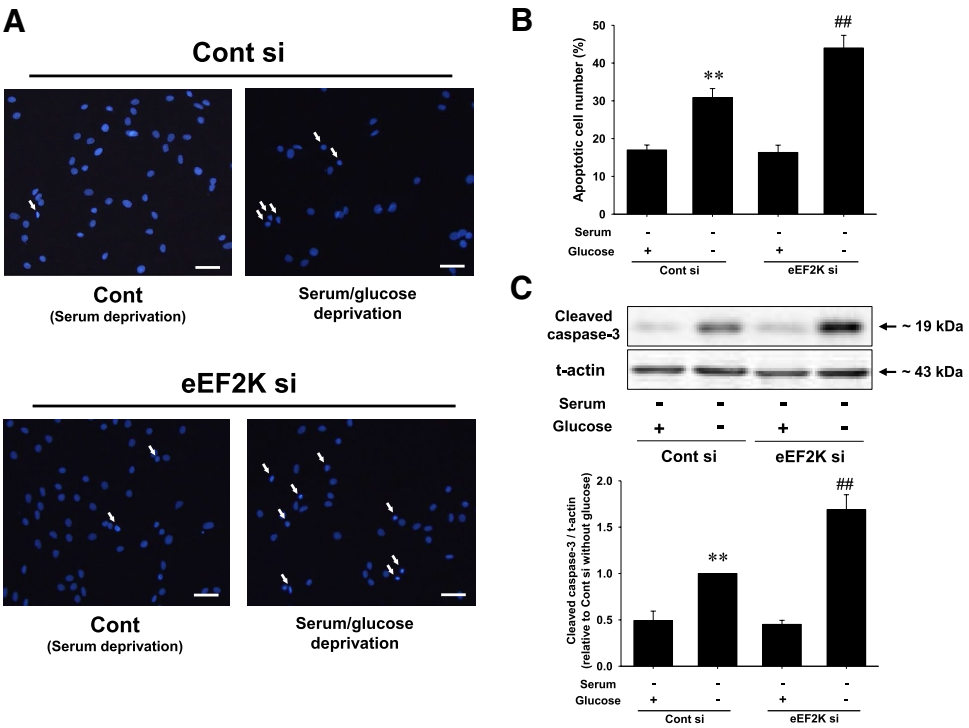

Fig. 3 Effects of eEF2K gene knockdown on GD-induced apoptosis in H9c2 cardiomyoblasts. After transfection with eEF2K or Cont siRNA, the cells were incubated with serum-free medium in the presence or absence of glucose for 24 h. To detect apoptotic nuclear condensation, the cells were treated with 4′, 6-diamidino-2-phenylindole (DAPI). Representative images for DAPI staining were shown (**A**; n = 5, arrows indicate condensed nuclei). Scale bar: 100 μm. Number of the condensed nucleus was counted, and the ratio to total cell nuclei (shown in %) was calculated (**B**; n = 5). After extraction of proteins, expression levels of cleaved caspase-3 were determined by Western blotting. Cleaved caspase-3 was normalized to t-actin. The result was shown as fold increase relative to Cont si without glucose (**C**; n = 6). $^{**}P < 0.01$ vs. Cont si with glucose, $^{\#\#}P < 0.01$ vs. Cont si without glucose

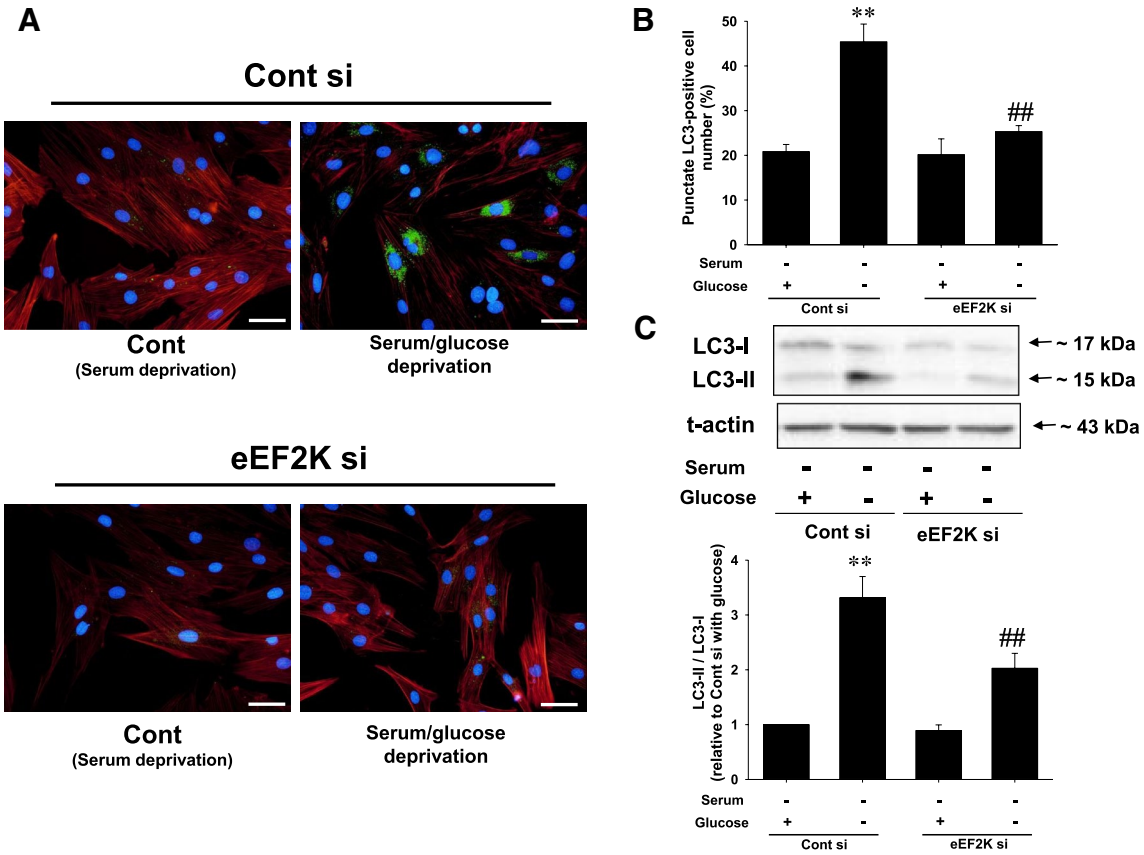

Fig. 4 Effects of eEF2K gene knockdown on GD-induced autophagy in H9c2 cardiomyoblasts. After transfection with eEF2K or Cont siRNA, the cells were incubated with serum-free medium in the presence or absence of glucose for 12 h. Autophagosome formation was examined by an immunofluorescence staining using a specific antibody against LC3. The cytoskeleton or nucleus was stained with rhodamine-phalloidin (red) or DAPI (blue), respectively. Autophagosome was expressed as LC3-positive green fluorescent dots (punctate LC3), and the cell with > 10 punctate LC3 was regarded as an autophagic cell. Representative images of autophagosome formation were shown (**A**; n = 3). Scale bar: 50 μm. Number of autophagic cell was counted and the ratio to total cell number (shown in %) was calculated (**B**; n > 100 cells in > 10 fields from each stimulation of three independent experiments). After extraction of proteins, expression levels of LC3 were determined by Western blotting. Ratio of LC3-II to LC3-I was measured as a quantitative index of autophagy. The result was shown as fold increase relative to Cont si with glucose (**C**; n = 5). $^{**}P < 0.01$ vs. Cont si with glucose, $^{\#\#}P < 0.01$ vs. Cont si without glucose

of eEF2 induced by eEF2K gene knockdown leads to the augmentation of GD-induced apoptosis and/or inhibition of autophagy. We confirmed that eEF2 specific siRNA decreased eEF2 protein expression (n = 4, Fig. 5A). It was conformed that eEF2K gene knockdown significantly increased the cleavage of caspase-3 (GD 24 h; n = 5–6, P < 0.05, Fig. 5B), which was significantly reversed by eEF2 gene knockdown (n = 5, P < 0.01, Fig. 5B). On the other hand, it was conformed that eEF2K gene knockdown significantly decreased the LC3-II to LC3-I ratio (GD 12 h; n = 6–8, P < 0.05, Fig. 5C), which was significantly reversed by eEF2 gene knockdown (n = 6–8, P < 0.01, Fig. 5C). Augmentation of autophagy by a pharmacological intervention was reported to attenuate doxorubicin-induced apoptosis in H9c2 cells [19]. Therefore, we tested whether 3-MA or Baf A1, an inhibitor of autophagy, increases GD-induced cleavage of caspase-3. It was conformed that GD (24 h) significantly increased cleavage of caspase-3 (n = 5–7, P < 0.05, Fig. 6A, n = 4–6, P < 0.01, Supplementary Fig. 3), which was significantly augmented by either 3-MA (n = 5–7, P < 0.01, Fig. 6A) or Baf A1 (n = 4–6, P < 0.01, Supplementary Fig. 3). We confirmed that 3-MA decreased GD-induced increase of LC3-II to LC3-I ratio (n = 5–7, Fig. 6A).

eEF2K/eEF2 axis under GD condition increases autophagy via AMPKα/ULK1 signaling

In starved condition including GD, AMPKα is activated and plays an important role in cellular energy homeostasis. It is also known that AMPKα promotes autophagy via phosphorylating ULK1 [20]. It was confirmed in control siRNA-transfected cells that GD (12 h) significantly

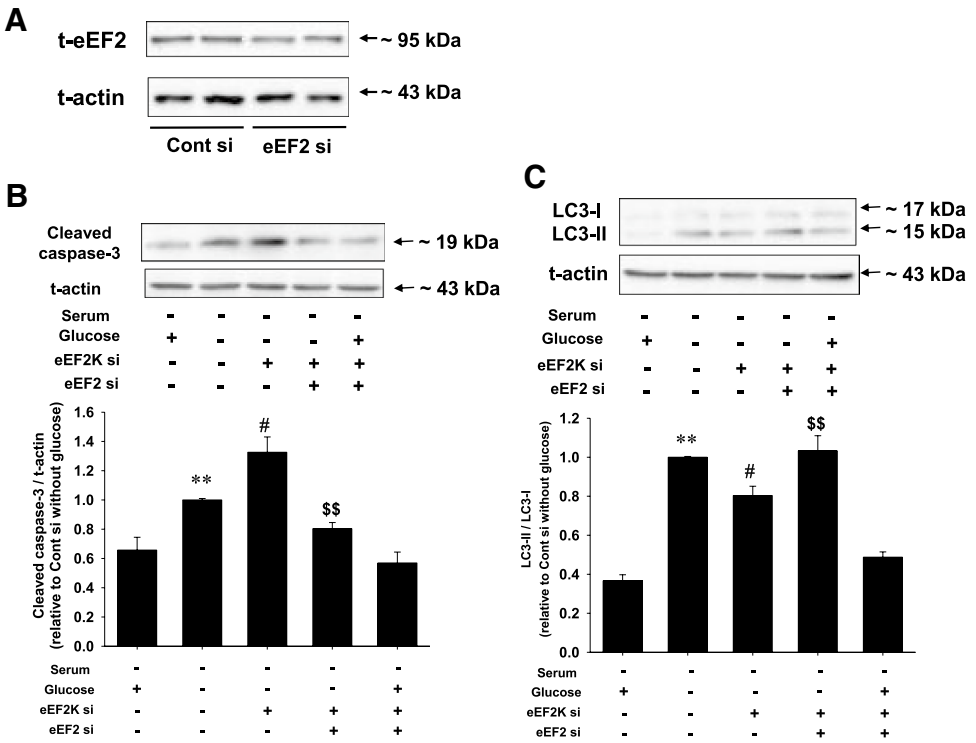

Fig. 5 eEF2K/eEF2 axis under GD condition regulates the signals related to apoptosis and autophagy in H9c2 cardiomyoblasts. After transfection with a specific siRNA against eEF2 (eEF2 si) or Cont siRNA for 24 h, proteins were extracted. Expression levels of t-eEF2 were determined by Western blotting. Equal protein loading was confirmed using t-actin antibody. Representative blot image was shown (**A**; n = 5). After transfection with siRNA against eEF2K alone, both of eEF2K and eEF2 or Cont, the cells were incubated with serum-free medium in the presence or absence of glucose for 12–24 h. After extraction of proteins, expression levels of cleaved caspase-3 (GD 24 h, n = 5–6; **B**) or LC3 (GD 12 h, n = 6–8; **C**) were determined by Western blotting. Cleaved caspase-3 was normalized to t-actin. Ratio of LC3-II to LC3-I was measured as a quantitative index of autophagy. These results were shown as fold increase relative to Cont si without glucose. $^{**}P < 0.01$ vs. Cont si with glucose, $^{\#}P < 0.05$ vs. Cont si without glucose, $^{\$\$}P < 0.01$ vs. eEF2K si without glucose

increased phosphorylation of AMPKα (n = 5, $P < 0.05$, Fig. 6B) and ULK1 (n = 5, $P < 0.01$, Fig. 6B), which was significantly inhibited by eEF2K gene knockdown (n = 5, AMPKα: $P < 0.05$; ULK1: $P < 0.01$, Fig. 6B). In addition, we confirmed in control siRNA-transfected cells that GD (12 h) increased phosphorylation of ACC, a well-established downstream substrate for AMPK (n = 5, Fig. 6B), indicating that AMPK was active, which was also inhibited by eEF2K gene knockdown (n = 5, Fig. 6B). We next investigated the effects of an inhibitor of AMPK, dorsomorphin on GD-induced autophagy. GD (12 h) significantly increased LC3-II to LC3-I ratio (n = 5, $P < 0.01$, Fig. 6C), which was significantly inhibited by dorsomorphin (n = 5, $P < 0.01$, Fig. 6C). It was conformed that GD (12 h) significantly increased phosphorylation of AMPKα (n = 5, $P < 0.05$, Supplementary Fig. 4) as well as its downstream substrates including ACC and ULK1 (n = 5, $P < 0.01$, Supplementary Fig. 4), which was significantly inhibited by dorsomorphin (n = 5, $P < 0.01$, Supplementary Fig. 4).

Discussion

Cardiac hypertrophy is one of the compensation mechanisms against the circulatory insufficiency including pressure and volume overload. However, coronary microvascular rarefaction and the following deprivation of nutrient including glucose in cardiomyocytes are caused during the development of cardiac hypertrophy, which results in cardiomyocyte death [4, 5]. Protein translation is a highly energy consuming process, which promotes cell death under nutrient-deprived condition. Activated eEF2K inhibits protein translation through phosphorylating (inactivating) its specific substrate eEF2. We previously showed that eEF2K activation and the following eEF2 phosphorylation were increased in the isolated heart from cardiac hypertrophy animal models [12]. In the present study, we thus tested the hypothesis that the eEF2K/eEF2 axis plays protective roles in rat cardiomyoblast death under GD condition.

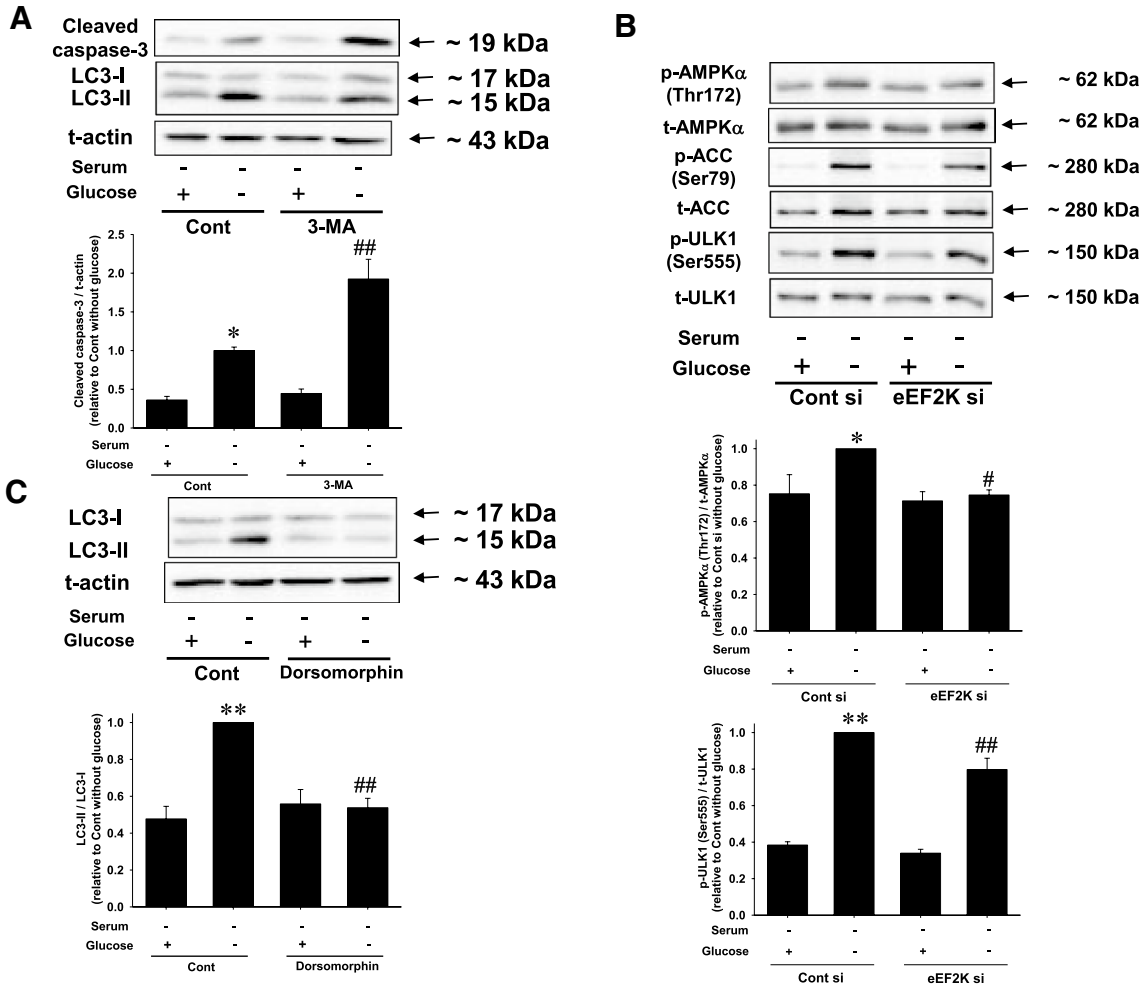

Fig. 6 eEF2K/eEF2 axis plays an inhibitory role against GD-induced apoptosis via the promotion of autophagy through adenosine monophosphate-activated protein kinase (AMPK)α/unc-51 like autophagy activating kinase (ULK)1 signaling in H9c2 cardiomyoblasts. After H9c2 cardiomyoblasts cultured with serum-free medium were treated with 3-methyladenine (3-MA; 2 mM) in the presence or absence of glucose for 24 h, proteins were extracted. Expression levels of cleaved caspase-3 and LC3 were determined by Western blotting. Representative blot image for LC3 was shown (n = 5–7; **A**). Cleaved caspase-3 was normalized to t-actin. The result was shown as fold increase relative to Cont (serum-free medium, a solvent of 3-MA-treatment) without glucose (n = 5–7; **A**). $^{*}P < 0.05$ vs. Cont with glucose, $^{\#\#}P < 0.01$ vs. Cont without glucose. After transfection with eEF2K siRNA or Cont siRNA, the cells were incubated with serum-free medium in the presence or absence of glucose for 12 h. After extraction of proteins, expression levels of AMPKα, acetyl-CoA carboxylase (ACC) or ULK1 were determined by Western blotting. Phospho-AMPKα (p-AMPKα) or phospho-ULK1 (p-ULK1) was normalized to total-AMPKα (t-AMPKα) or total-ULK1 (t-ULK1), respectively. Representative blot images for phospho (p-ACC)- and total (t-ACC)-ACC were shown (n = 5; **B**). The results were shown as fold increase relative to Cont si without glucose (n = 5; **B**). $^{*}P < 0.05$ vs. Cont si with glucose, $^{**}P < 0.01$ vs. Cont si with glucose, $^{\#}P < 0.05$ vs. Cont si without glucose, $^{\#\#}P < 0.01$ vs. Cont si without glucose. After H9c2 cells cultured with serum-free medium were treated with dorsomorphin (5 μM) in the presence or absence of glucose for 12 h, proteins were extracted. Expression levels of LC3 were determined by Western blotting. Ratio of LC3-II to LC3-I was measured as a quantitative index of autophagy. The result was shown as fold increase relative to Cont (dimethyl sulfoxide, a solvent of dorsomorphin-treatment) without glucose (n = 5, **C**). $^{**}P < 0.01$ vs. Cont with glucose, $^{\#\#}P < 0.01$ vs. Cont without glucose

We showed that GD significantly increased eEF2 phosphorylation (Fig. 1A) and H9c2 cell death (Fig. 1D, E). eEF2K gene knockdown decreased GD-induced eEF2 phosphorylation (Fig. 2A), indicating an eEF2 activation, which was followed by an augmentation of cell death induced by GD (Fig. 2B). These results suggest that eEF2 phosphorylation contributes to increase in cell viability under GD condition. It was reported that tumor cells having abundant activated eEF2K show resistance to nutrient deprivation via blocking protein translation through phosphorylating eEF2 [11], which is in accordance with the present results.

We also showed that GD significantly increased apoptotic nuclear condensation (Fig. 3A, B) and expression of cleaved caspase-3 (Figs. 1C, 3C), which were significantly

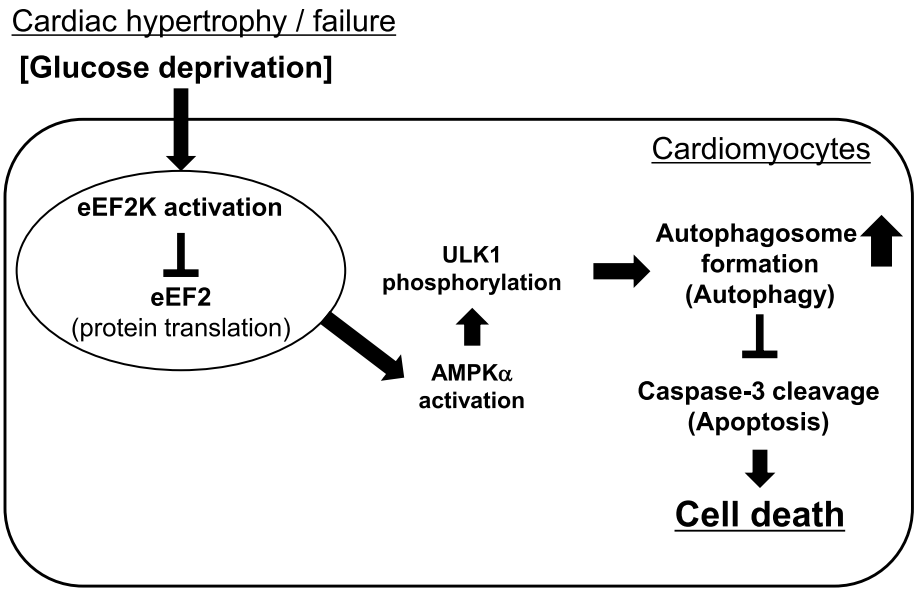

Fig. 7 Summary of the present results. eEF2K/eEF2 axis mediates the inhibition of caspase-3-dependent apoptotic cell death at least in part via the promotion of autophagy through AMPKα/ULK1 signaling pathway in glucose-deprived H9c2 cardiomyoblasts. These results indicate that eEF2K/eEF2 has protective roles in the pathogenesis of cardiac hypertrophy and failure accompanied by glucose-deprived cardiomyocytes

augmented by eEF2K gene knockdown (Fig. 3 and Supplementary Fig. 2). In addition, GD significantly promoted autophagosome formation (Fig. 4A, B). GD increased LC3-II to LC3-I ratio (Figs. 1B, 4C, Supplementary Fig. 1), which was augmented by an inhibitor of autophagy, Baf A1 (Supplementary Fig. 1), indicating the promotion of autophagic flux. GD-induced increase of LC3-II to LC3-I ratio was significantly inhibited by eEF2K gene knockdown (Fig. 4). Autophagy is a highly conserved intracellular process for protein degradation and recycling. Sishi et al. [19] reported that augmentation of autophagy by a pharmacological intervention attenuates doxorubicin-induced apoptosis in H9c2 cells. In this study, an inhibitor of autophagy, 3-MA (Fig. 6A) or Baf A1 (Supplementary Fig. 3) significantly augmented the GD-induced cleavage of caspase-3. We also showed that eEF2 gene knockdown significantly reversed both the augmentation of GD-induced apoptosis (Fig. 5B) and the inhibition of autophagy (Fig. 5C) induced by eEF2K gene knockdown. Our results collectively suggest that eEF2K/eEF2 axis mediates the inhibition of apoptosis at least in part via the promotion of autophagy under GD condition.

AMPKα is one of the intracellular energy sensors, which is also known as a positive regulator of autophagy [20]. AMPKα was reported to promote the initiation of autophagy via upregulating the signals related to autophagosome formation including ULK1 [21] and class III phosphatidylinositol-3 kinase/Beclin1 complex [22]. In the present study, we showed that GD significantly increased phosphorylation of AMPKα and ULK1, which was significantly inhibited by eEF2K gene knockdown (Fig. 6B). Moreover, an AMPK inhibitor, dorsomorphin (5 μM) significantly inhibited GD-induced phosphorylation of ULK1 (Supplementary Fig. 4) and increase of LC3-II to LC3-I ratio (Fig. 6C). The results suggest that eEF2K/eEF2 axis under GD condition mediates the promotion of autophagy at least in part via AMPKα/ULK1 signaling. However, the mechanisms underlying eEF2K/eEF2 regulation of AMPK activation remain unknown. Liver kinase B1 (LKB1) is one of upstream kinases for AMPK [23]. Recent study revealed the novel mechanisms for activating AMPK under GD condition in both AMP- and adenosine diphosphate (ADP)-independent manners [24]. GD rapidly decreases intracellular levels of fructose-1,6-bisphosphate (FBP), and its upstream enzyme aldolase is unoccupied by FBP. The unoccupied aldolase mediates the changes in vacuolar ATPase/Ragulator complex on the surface of lysosome. The complex subsequently provides docking site for AXIN/LKB1 complex, which leads to the LKB1-induced AMPK activation [24, 25]. It might be possible in this study that eEF2K/eEF2 regulation of protein translation and/or energy consumption under GD condition might control AMPK activation via affecting the above AMP/ADP-independent pathways. Further investigations for exploring the detailed mechanisms are necessary. On the other hand, eEF2K contributed to protect the tumor cells from nutrient deprivation through other mechanisms including inhibition of energy consumption [11, 26] than promoting autophagy. In addition, AMPK has protective roles against cardiomyocyte death via autophagy-independent mechanisms including activation of endothelial nitric oxide synthase [27] and antioxidative molecule, Nrf-2 [28] in energy-starved condition. In this study, eEF2K might thus inhibit H9c2 cell death under GD condition not only through promotion of autophagy, but also through autophagy-independent mechanisms.

In conclusion, we for the first time revealed that eEF2K/eEF2 axis mediates the inhibition of caspase-3-dependent apoptosis at least in part via the promotion of autophagy

through AMPKα/ULK1 signaling pathway in the glucose-deprived cardiomyoblasts (Fig. 7). These results indicate that eEF2K/eEF2 has protective roles in the pathogenesis of cardiac hypertrophy and failure accompanied by glucose-deprived cardiomyocytes.

Acknowledgements This study was supported by the Grant for Scientific Research from Japan Society for Promotion of Science (JSPS KAKENHI Grant Number JP16J08307), NISHINOMIYA Basic Research Fund and Kato Memorial Bioscience Foundation, Japan.

Compliance with ethical standards

Conflict of interest The authors declare that they have no conflict of interest.

References

1. Messerli FH, Rimoldi SF, Bangalore S (2017) The transition From hypertension to heart failure: contemporary update. JACC Heart Fail 5:543–551. https://doi.org/10.1016/j.jchf.2017.04.012
2. Carabello BA (2001) Progress in mitral and aortic regurgitation. Prog Cardiovasc Dis 43:457–475. https://doi.org/10.1053/pcad.2001.24597
3. Braunwald E (2017) Cardiomyopathies: an overview. Circ Res 121:711–721. https://doi.org/10.1161/CIRCRESAHA.117.311812
4. González A, Ravassa S, Beaumont J et al (2011) New targets to treat the structural remodeling of the myocardium. J Am Coll Cardiol 58:1833–1843. https://doi.org/10.1016/j.jacc.2011.06.058
5. Oka T, Akazawa H, Naito AT, Komuro I (2014) Angiogenesis and cardiac hypertrophy: maintenance of cardiac function and causative roles in heart failure. Circ Res 114:565–571. https://doi.org/10.1161/CIRCRESAHA.114.300507
6. Iurlaro R, Püschel F, León-Annicchiarico CL et al (2017) Glucose deprivation induces ATF4-mediated apoptosis through TRAIL death receptors. Mol Cell Biol 37:e00479–e00416. https://doi.org/10.1128/MCB.00479-16
7. Bialik S, Cryns VL, Drincic A et al (1999) The mitochondrial apoptotic pathway is activated by serum and glucose deprivation in cardiac myocytes. Circ Res 85:403–414
8. Jang BG, Choi BY, Kim JH et al (2013) Impairment of autophagic flux promotes glucose reperfusion-induced neuro2A cell death after glucose deprivation. PLoS ONE 8:e76466. https://doi.org/10.1371/journal.pone.0076466
9. Yang Y-H, Chen K, Li B et al (2013) Estradiol inhibits osteoblast apoptosis via promotion of autophagy through the ER-ERK-mTOR pathway. Apoptosis 18:1363–1375. https://doi.org/10.1007/s10495-013-0867-x
10. Kaul G, Pattan G, Rafeequi T (2011) Eukaryotic elongation factor-2 (eEF2): its regulation and peptide chain elongation. Cell Biochem Funct 29:227–234. https://doi.org/10.1002/cbf.1740
11. Leprivier G, Remke M, Rotblat B et al (2013) The eEF2 kinase confers resistance to nutrient deprivation by blocking translation elongation. Cell 153:1064–1079. https://doi.org/10.1016/j.cell.2013.04.055
12. Kameshima S, Okada M, Ikeda S et al (2016) Coordination of changes in expression and phosphorylation of eukaryotic elongation factor 2 (eEF2) and eEF2 kinase in hypertrophied cardiomyocytes. Biochem Biophys Rep 7:218–224. https://doi.org/10.1016/j.bbrep.2016.06.018
13. Kanazawa H, Imoto K, Okada M, Yamawaki H (2017) Canstatin inhibits hypoxia-induced apoptosis through activation of integrin/focal adhesion kinase/Akt signaling pathway in H9c2 cardiomyoblasts. PLoS ONE 12:e0173051. https://doi.org/10.1371/journal.pone.0173051
14. Sakamoto Y, Kameshima S, Kakuda C et al (2017) Visceral adipose tissue-derived serine protease inhibitor prevents the development of monocrotaline-induced pulmonary arterial hypertension in rats. Pflugers Arch 469:1425–1432. https://doi.org/10.1007/s00424-017-2043-6
15. Kazama K, Okada M, Yamawaki H (2014) A novel adipocytokine, omentin, inhibits monocrotaline-induced pulmonary arterial hypertension in rats. Biochem Biophys Res Commun 452:142–146. https://doi.org/10.1016/j.bbrc.2014.08.070
16. Yasuda J, Okada M, Yamawaki H (2017) T3 peptide, an active fragment of tumstatin, inhibits H2O2-induced apoptosis in H9c2 cardiomyoblasts. Eur J Pharmacol 807:64–70. https://doi.org/10.1016/j.ejphar.2017.04.032
17. Lu Z, Chen C, Wu Z et al (2017) A dual role of P53 in regulating colistin-induced autophagy in PC-12 cells. Front Pharmacol 8:768. https://doi.org/10.3389/fphar.2017.00768
18. Wang X, Xie J, Proud C (2017) Eukaryotic elongation factor 2 kinase (eEF2K) in cancer. Cancers (Basel) 9:162. https://doi.org/10.3390/cancers9120162
19. Sishi BJN, Loos B, van Rooyen J, Engelbrecht A-M (2013) Autophagy upregulation promotes survival and attenuates doxorubicin-induced cardiotoxicity. Biochem Pharmacol 85:124–134. https://doi.org/10.1016/j.bcp.2012.10.005
20. Ha J, Guan K-L, Kim J (2015) AMPK and autophagy in glucose/glycogen metabolism. Mol Aspects Med 46:46–62. https://doi.org/10.1016/j.mam.2015.08.002
21. Egan DF, Shackelford DB, Mihaylova MM et al (2011) Phosphorylation of ULK1 (hATG1) by AMP-activated protein kinase connects energy sensing to mitophagy. Science 331:456–461. https://doi.org/10.1126/science.1196371
22. Kim J, Guan K-L (2013) AMPK connects energy stress to PIK3C3/VPS34 regulation. Autophagy 9:1110–1111. https://doi.org/10.4161/auto.24877
23. Gan R-Y, Li H-B (2014) Recent progress on liver kinase B1 (LKB1): expression, regulation, downstream signaling and cancer suppressive function. Int J Mol Sci 15:16698–16718. https://doi.org/10.3390/ijms150916698
24. Zhang C-S, Hawley SA, Zong Y et al (2017) Fructose-1,6-bisphosphate and aldolase mediate glucose sensing by AMPK. Nature 548:112–116. https://doi.org/10.1038/nature23275
25. Lin S-C, Hardie DG (2018) AMPK: sensing glucose as well as cellular energy status. Cell Metab 27:299–313. https://doi.org/10.1016/j.cmet.2017.10.009
26. Moore CEJ, Wang X, Xie J et al (2016) Elongation factor 2 kinase promotes cell survival by inhibiting protein synthesis without inducing autophagy. Cell Signal 28:284–293. https://doi.org/10.1016/j.cellsig.2016.01.005
27. Calvert JW, Gundewar S, Jha S et al (2008) Acute metformin therapy confers cardioprotection against myocardial infarction via AMPK-eNOS-mediated signaling. Diabetes 57:696–705. https://doi.org/10.2337/db07-1098
28. Wu W-Y, Li Y-D, Cui Y-K et al (2018) The natural flavone acacetin confers cardiomyocyte protection against hypoxia/reoxygenation injury via AMPK-mediated activation of Nrf2 signaling pathway. Front Pharmacol 9:497. https://doi.org/10.3389/fphar.2018.00497